*J. Microbiol. Biotechnol.* (2011), **21**(9), 903–913
doi: 10.4014/jmb.1104.04044
First published online 18 July 2011

JOURNAL OF MICROBIOLOGY AND BIOTECHNOLOGY



# Cell Death Mediated by *Vibrio parahaemolyticus* Type III Secretion System 1 Is Dependent on ERK1/2 MAPK, but Independent of Caspases

**Yang, Yu Jin, Na Kyung Lee, Na Yeon Lee, Jong Woong Lee, and Soon-Jung Park***

*Department of Environmental Medical Biology and Institute of Tropical Medicine, The Brain Korea 21 Project, Yonsei University College of Medicine, Seoul 120-752, Korea*

Received: April 27, 2011 / Accepted: June 13, 2011

***Vibrio parahaemolyticus*, which causes gastroenteritis, wound infection, and septicemia, has two sets of type III secretion systems (TTSS), TTSS1 and TTSS2. A TTSS1-deficient *vcrD1* mutant of *V. parahaemolyticus* showed an attenuated cytotoxicity against HEp-2 cells, and a significant reduction in mouse lethality, which were both restored by complementation with the intact *vcrD1* gene. *V. parahaemolyticus* also triggered phosphorylation of mitogen-activated protein kinases (MAPKs) including p38 and ERK1/2 in HEp-2 cells. The ability to activate p38 and ERK1/2 was significantly affected in a TTSS1-deficient *vcrD1* mutant. Experiments using MAPK inhibitors showed that p38 and ERK1/2 MAPKs are involved in *V. parahaemolyticus*-induced death of HEp-2 cells. In addition, caspase-3 and caspase-9 were processed into active forms in *V. parahaemolyticus*-exposed HEp-2 cells, but activation of caspases was not essential for *V. parahaemolyticus*-induced death of HEp-2 cells, as shown by both annexin V staining and lactate dehydrogenase release assays. We conclude that secreted protein(s) of TTSS1 play an important role in activation of p38 and ERK1/2 in HEp-2 cells that eventually leads to cell death *via* a caspase-independent mechanism.**

**Keywords:** *Vibrio parahaemolyticus*, mitogen-activated protein kinases, caspases

*Vibrio parahaemolyticus* is a Gram-negative bacterium commonly found in marine and estuarine environments [8]. Infections with *V. parahaemolyticus* arise from the consumption of raw or undercooked shellfish and typically result in gastroenteritis that can be life-threatening to individuals who are immunocompromised or have pre-existing medical conditions such as liver disease or diabetes [18, 20].

A distinct characteristic of clinical *V. parahaemolyticus* strains is the production of thermostable direct hemolysin (TDH) [10]. TDH is one of the important virulence factors of this bacterium, because purified TDH elicits a number of biological effects including erythrocyte lysis, cardiotoxicity, chloride ion secretion, and fluid accumulation in the ileal loop model [19, 24–27]. However, *V. parahaemolyticus* strains that lack the TDH and TDH-related hemolysin retain cytotoxicity in infection models using tissue cultures, indicating the presence of other cytotoxic factor(s) in this pathogen [14, 23].

The type III secretion system (TTSS) present in several Gram-negative pathogens is also a determinant of virulence since this bacterial machinery delivers effectors of *V. parahaemolyticus* into the host cells, resulting in modulation of host components including the cytoskeleton and signal transduction [11]. Whereas the genes encoding the secretion apparatus are conserved, genes encoding effectors are unique to different microorganisms [28]. Genome sequencing of *V. parahaemolyticus* RIMD2210633 has revealed two sets of TTSS, TTSS1 and TTSS2 [15]. TTSS1 is similar to the Ysc secretion system of *Yersinia*, whereas TTSS2 shows homology with the Inv-Mxi-Spa secretion systems of *Salmonella* and *Shigella.* Investigations using mutant *V. parahaemolyticus* lacking TDH and one of the TTSSs, indicated that TTSS1 plays an important role in cytotoxicity against tissue culture cells, whereas TTSS2 is associated with bacterial enterotoxicity in the rabbit ileal loop model [15, 23].

Among the components of *V. parahaemolyticus* TTSS1, VcrD1 protein is the most highly conserved compared with those of other bacteria, ranging from 41% identity with MxiA of *S. flexneri* to 94% identity with EscV of *V. harveyi.* Based on the structure of *Yersinia* TTSS, VcrD is predicted to be an inner membrane protein comprising the

*Corresponding author
Phone: +82-2-2228-1843; Fax: +82-2-363-8676;
E-mail: sjpark615@yuhs.ac

TTSS1 apparatus (http://www.genome.jp). In this study, we constructed a TTSS1-deficient *V. parahaemolyticus* strain with intact TDHs by directed mutagenesis of the *vcrD1* gene, and used this strain to determine the role of TTSS1 in *V. parahaemolyticus*-induced death of HEp-2 cells. In addition, we defined the roles of two host signaling pathways, caspases and MAPKs, in *V. parahaemolyticus*-induced death of HEp-2 cells.

## Materials and Methods

### Bacterial Strains, Plasmids, and Culture Conditions

The strains and plasmids used in this study are listed in Table 1. *Escherichia coli* strains used for plasmid DNA preparation and the conjugational transfer of plasmid were grown in Luria–Bertani (LB) broth (1% bacto-tryptone, 0.5% yeast extract, and 1% NaCl) or on LB plate containing 1.5% agar. *V. parahaemolyticus* RIMD2210633 (ATCC number BAA-238) was used as the wild-type in this study, and was cultured in LB medium supplemented with additional 2% NaCl (LBS). Ampicillin was added to the medium at 100 μg/ml for the maintenance of plasmids in *E. coli*. Chloramphenicol at a concentration of 2 μg/ml was used for selection of *V. parahaemolyticus* exconjugants. All medium components were purchased from Difco (Lowrence, KS, USA), and the chemicals and antibiotics were from Sigma (St. Louis, MO, USA).

### Cultivation of Cell Lines

HEp-2 cell line (ATCC No. CCL-23) derived from human epithelial cells was cultured in Dulbecco's modified Eagle's medium (DMEM; Gibco BRL, Karsruhe, Germany) supplemented with 10% fetal bovine serum (FBS), 2 mM L-glutamine, 100 U/ml penicillin G, and 100 μg/ml streptomycin. The cells were maintained at 37°C in a humidified atmosphere containing 5% $CO_2$. FBS and DMEM were obtained from Hyclone (Logan, UT, USA).

### Construction of *ΔvcrD1 V. parahaemolyticus*, NK-1, and Complementation Strain

Chromosomal DNA isolated from *V. parahaemolyticus* RIMD2210633 was used as the template for PCR. A 704 bp *vcrD1* upstream region was amplified using the primers VP1662A (5'-GATCGAGCTCCAT TGAAGCCTTTACTCACGT-3') and VP1662B (5'-GATCCTGCAG TCAACTTATTCATGAGATTC-3'). The resultant PCR product was digested with the appropriate restriction enzymes, *Sac*I and *Pst*I, and ligated to plasmid pBluescript SKII (+) to produce pSKvcrD1up. A 702 bp DNA fragment was amplified using primers VP1662C (5'-GATCCTGCAGTTGGACGGGTAGGGATGTAA-3') and VP1662D (5'-GATCGGGCCCT GCCTGCGGCGCTGAACTTC-3'), which is located downstream of the *vcrD1* open reading frame (ORF). This PCR product was digested with *Pst*I and *Apa*I, and cloned into pSKvcrD1up, resulting in pSKvcrD1updown. Finally, a 1.4 kb DNA fragment of pSKvcrD1updown was inserted into the *Sac*I and *Apa*I sites of pDM4 [17] to yield pDMΔvcrD1. Plasmid pDMΔvcrD1 in the SM10 λ*pir* strain [16] was mobilized to *V. parahaemolyticus* RIMD2210633, and the exconjugants were selected by plating the conjugation mixture of *E. coli* and *V. parahaemolyticus* on thiosulfate citrate bile sucrose (TCBS) agar plates supplemented with 2 μg/ml of chloramphenicol. A colony with characteristics indicating a double homologous recombination event (resistance to 10% sucrose, and sensitivity to chloramphenicol) was further confirmed by PCR using primers VP1622A and VP1622D, and the corresponding mutant strain was named NK-1 (Fig. 1A).

A 2,186 bp DNA fragment containing an ORF and a 36 bp upstream region of the *vcrD1* gene was amplified from *V. parahaemolyticus* genomic DNA using two primers, VP1662E (5'-CGGCCGCCAAG CGCATCGACGCTATC-3') and VP1662F (5'-GGGGTACCGATTG TACAAGTGCTGCGTTC-3'). This DNA fragment was cloned into

**Table 1.** Bacterial strains and plasmids used in this study.

| Strains or plasmids | Relevant characteristics | Source, reference |
|---|---|---|
| *E. coli* | | |
| DH5α | *supE44 ΔlacU169* (Φ80 *lacZ ΔM15*) *hsdR17 recA1 endA1 gyrA96 thi-1 relA1* | Laboratory collection |
| SM10 λ*pir* | *thi thr leu tonA lacy supE recA*::RP4-2-Tc::Mu λ*pir*, OriT of RP4 $Km^r$; conjugational donor | [16] |
| BL21 (DE3) | *E. coli* B $F^-$ *dcm ompT hsdS* ($rB^-$ $mB^-$) *gal* λ (DE3) | Invitrogen |
| *V. parahaemolyticus* | | |
| RIMD2210633 | Kanagawa phenotype-positive, serotype O3:K6 | ATCC |
| NK1 | *ΔvcrD1* mutant derived from RIMD2210633 | This study |
| Plasmids | | |
| pBluescript SKII (+) | Cloning vector, $Ap^r$, *lac* promoter (*lacZ*), f1, ColE1 | Stratagene |
| pSKvcrD1up | pBluescript SK II (+), 704-bp upstream of *vcrD1* | This study |
| pSKvcrD1updown | pSKvcrD1up, 702 bp downstream of *vcrD1* | This study |
| pDM4 | Suicide vector, OriR6K $Cm^r$ | [17] |
| pDMΔvcrD1 | pDM4, 1,406 bp *ΔvcrD1* DNA fragment | This study |
| pRK415 | Broad-host-range plasmid, $Tc^r$ | [12] |
| pRKvcrD1 | pRK415, 1,035 bp $vcrD1^+$ | This study |
| pET32a | Expression vector for histidine-tagged protein | Novagen |
| pETvopQ | pET32a, 1,480 bp $vopQ^+$ | This study |

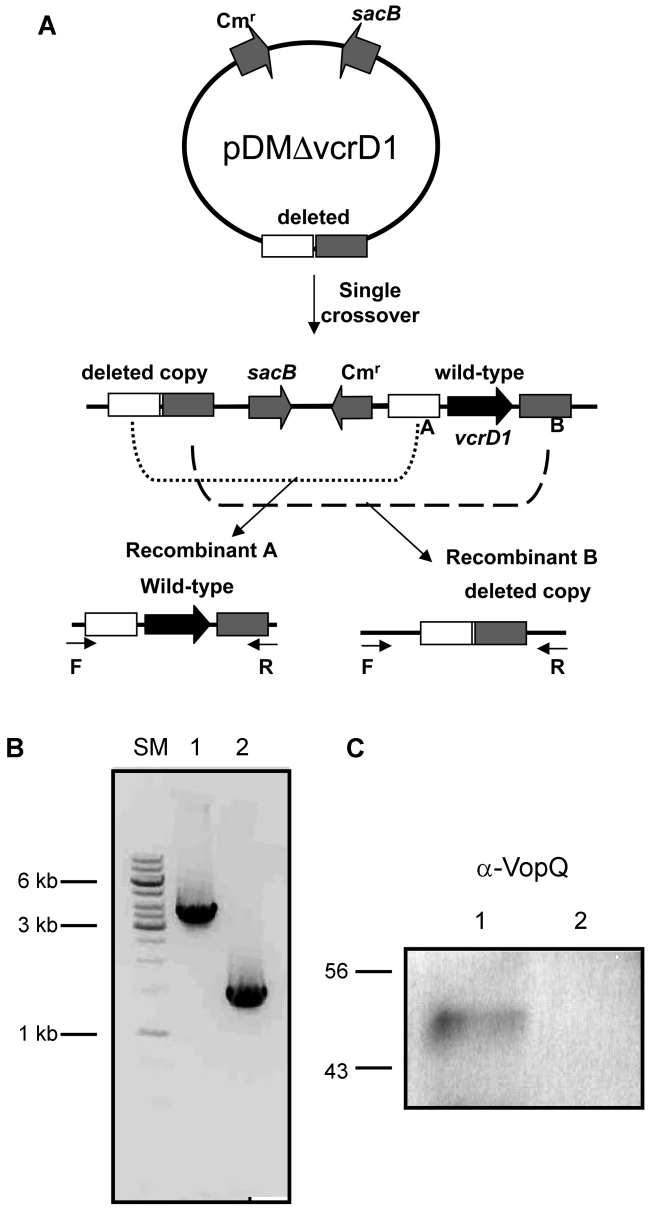


**Fig. 1.** Confirmation of *ΔvcrD1 V. parahaemolyticus* strain, NK1.

**A**. A suicide plasmid containing upstream and downstream regions of the *vcrD1* gene was constructed and used to generate a *ΔvcrD1* mutant of *V. parahaemolyticus via* an allelic exchange of the *ΔvcrD1* region with the homologous region of the *V. parahaemolyticus* chromosome. **B**. The adjacent region of the *vcrD1* locus was amplified from wild-type (lane 1) and *ΔvcrD1 V. parahaemolyticus* (lane 2) by PCR using primers, VP1622A and VP1622D. SM represents the DNA size marker, 1 kb DNA ladder. **C**. Western blot analysis of secretomes of wild-type (lane 1) and NK1, the *ΔvcrD1 V. parahaemolyticus* (lane 2), using polyclonal Ab against VopQ, an effector of TTSS1.

a *Kpn*I/*Bam*HI-treated broad-host-range vector, pRK415, to produce pRKvcrD1. This *vcrD1*$^+$-containing plasmid was mobilized to the *V. parahaemolyticus* NK1 strain *via* conjugation. Wild-type carrying pRK415 and the NK1 strain carrying pRK415 were constructed in the same manner to serve as controls.

**Formation of Recombinant VopQ (VepA) Protein and its Specific Polyclonal Antibodies**

A 1,480 bp *vopQ* (*vepA*) DNA fragment was amplified with primers VP1680F (5'-CACCATGGTGAATACAACCTCAAAAA-3') and VP1680R (5'-AATCCAGCCTTCGGCTAAGTACATT-3') and cloned into pET32a (Novagen, Gibbstown, NJ, USA) to produce plasmid pETVopQ. Histidine-tagged recombinant VopQ (rVopQ), expressed in *E. coli* BL21 (DE3) with an addition of 0.1 mM isopropyl β-D-thiogalactoside (IPTG; Sigma, St. Louis, MO, USA), was used for immunization of a specific pathogen-free rat (CrjBgi:CD[SD]IGS, 7-week-old, female) to make polyclonal antibodies (Ab).

**Western Blot Analysis of Secreted Proteins from *V. parahaemolyticus***

Secreted proteins were prepared from wild-type and *ΔvcrD1 V. parahaemolyticus* strains cultivated in LBS broth at 37°C. Bacterial cells at an optimal density at 600 nm ($OD_{600}$) of 0.8 were centrifuged at 8,000 rpm for 15 min at 4°C, and the resultant supernatants were passed through a 0.2 μm pore membrane filter. Proteins were concentrated using centricon YM-10 (Millipore, Bedford, MA, USA) at 4°C.

Concentrated supernatants were prepared in sample buffer [50 mM Tris-HCl, pH 6.8, 100 mM dithiothreitol, 2% SDS, 0.1% bromophenol blue, and 20% (v/v) glycerol], separated by SDS–polyacrylamide gel electrophoresis (SDS–PAGE), and transferred to polyvinylidene fluoride (PVDF) membrane (Millipore, Bedford, MA, USA). Membranes were blocked with 3% (w/v) skim milk in Tris-buffered saline with Tween 20 (TBST; 150 mM NaCl, 50 mM Tris-HCl, and 0.1% Tween 20), and then incubated overnight at 4°C with Ab specific to VopQ (an effector secreted by the TTSS1) [1]. After incubation with horseradish peroxidase (HRP)-conjugated secondary Ab, immunoreactive bands were visualized using an enhanced chemiluminescence system (Cell Signaling Technology, Beverly, MA, USA).

**Cytotoxicity Assays**

HEp-2 cells were seeded at $1 \times 10^5$ cells per well into a 24-well plate and incubated overnight at 37°C. Before infection, HEp-2 cells were starved for 2 h in serum-free DMEM. The cells were co-cultured with bacteria at a multiplicity of infection (MOI) of 200 for various times up to 6 h. The release of lactate dehydrogenase (LDH) into the medium was assayed using the Cyto-Tox 96 nonradioactive cytotoxicity kit (Promega, Madison, WI, USA) according to the manufacturer's instructions. The LDH release (percent cytotoxicity) was calculated using the following equation: ($OD_{490}$ of experimental release – $OD_{490}$ of spontaneous release) / ($OD_{490}$ of maximum release – $OD_{490}$ of spontaneous release) × 100. The spontaneous release is the amount of LDH released from the cytoplasm of uninfected HEp-2 cells, and the maximum release is the amount of LDH released from HEp-2 cells treated with 1% Triton X-100.

For complementation strains, wild-type strain carrying pRK415, NK-1 carrying pRK415, and NK1 carrying pRKvcrD1, the supernatants of the HEp-2 cells infected at MOI 200 were harvested at 6 h and 8 h post-infection, and assayed for LDH release as described above.

Generation of apoptotic cells following exposure to *V. parahaemolyticus* was monitored using annexin V staining. HEp-2 cells were seeded at $1 \times 10^5$ cells per well in a 24-well plate and incubated overnight at 37°C. The cells were then co-cultured with various *V. parahaemolyticus* strains (wild-type, *ΔvcrD* mutant NK1, wild-type carrying pRK415, NK-1 carrying pRK415, and NK-1 carrying pRKvcrD1) for 6 h at MOIs 100 and 200. Apoptotic cells

were detected by staining with annexin V (BD Pharminogen, Palo Alto, CA, USA) at a final concentration of 2 μg/ml, and the degree of cell death was assessed using fluorescence-activated cell sorting (FACS) analysis. FACS analyses were performed on at least 10,000 cells per sample with a FACScan (Becton Dickinson, Franklin Lakes, NJ, USA).

**Mouse Lethality Experiment**

Specific-pathogen-free, 7-week-old female ICR mice (CrljOri:CD1[ICR]) were used to test the pathogenicity of various *V. parahaemolyticus* strains (wild-type, *ΔvcrD1* mutant NK1, wild-type carrying pRK415, NK1 carrying pRK415, and NK1 carrying pRKvcrD1). *V. parahaemolyticus* was grown overnight in LBS medium, freshly inoculated into the same medium, and harvested when bacterial growth reached an $OD_{600}$ of 0.8. One hundred μl of bacterial suspension containing $1 \times 10^8$ colony forming units (CFU) was prepared in phosphate-buffered saline (PBS) (1.44% $Na_2HPO_4$, 0.24% $KH_2PO_4$, 8% NaCl, and 0.2% KCl, pH 7.4), and injected intraperitoneally into 10 mice for each *V. parahaemolyticus* strain. The number of dead mice was monitored over a 20 h period after the injection of bacteria. The animals received humane care in accordance with our institutional guidelines and the legal requirements of Korea.

**Detection of MAPK and Caspase Activation in HEp-2 Cells by Western Blot Analysis**

HEp-2 cells were seeded at $5 \times 10^5$ cells per well in a 6-well plate and incubated overnight at 37°C. After starvation for 4 h in serum-free DMEM, the cells were co-cultured with PBS-washed bacteria (wild-type and *ΔvcrD1* mutant NK-1) at various MOIs (10, 50, 100, and 200) for 6 h. As a positive control for MAPK activation, HEp-2 cells were treated with UV at 200 mJ/cm$^2$ for 30 min. As a positive control for caspase activation, HEp-2 cells were incubated with 5 μM staurosporin (STS) for 30 min. The cells were then washed twice with ice-cold PBS, and treated with lysis buffer (Promega, Madison, WI, USA) for 30 min at 4°C. After centrifugation for 20 min at 13,000 rpm and 4°C, the supernatants were subjected to Western blot analysis to detect activation of MAPKs, caspase 3, and caspase 9.

Supernatant containing 20 μg of the total protein was separated by SDS−PAGE, and transferred onto a PVDF membrane. Membranes were blocked with 5% skim milk in TBST, and then incubated overnight at 4°C with primary Ab specific to phosphorylated p38, phosphorylated ERK1/2, phosphorylated JNK MAPK, caspase 3, or caspase 9. After incubation with HRP-conjugated secondary Ab, immunoreactive bands were visualized using an enhanced chemiluminescence system (Cell Signaling Technology, Beverly, MA, USA). Membranes were then incubated in a stripping buffer (100 mM 2-mercaptoethanol, 2% SDS, and 62.5 mM Tris-HCl, pH 6.7) at 56°C for 30 min, and probed with Ab against p38 MAPK, ERK1/2, or JNK. Rabbit polyclonal Abs against p38, phospho-p38, JNK, phospho-JNK, ERK1/2, phospho-ERK1/2, caspase 3, and caspase 9 were purchased from Cell Signaling Technology (Beverly, MA, USA). The level of β-actin in the cell extracts used for Western blot analysis was also determined as a loading control.

**Pretreatment of HEp-2 Cells with Various Inhibitors**

To investigate the roles of various signaling components in *V. parahaemolyticus*-induced cell death, HEp-2 cells were treated with selective inhibitor(s) prior to incubation with *V. parahaemolyticus* and their viabilities were compared with those of untreated cells using LDH assays as described above. The following inhibitors were purchased from Calbiochem (Schwalbach, Germany): z-VAD-FMK, a pan caspase inhibitor; SB202190, a selective inhibitor of p38 MAPK; SP600125, a selective inhibitor for JNK; and PD98059, an inhibitor of MAPK kinase.

HEp-2 cells were pretreated for 30 min with each of the following inhibitors at the indicated concentrations; z-VAD-FMK at 1−100 μM, SB202190 at 1−20 μM, SP600125 at 1−20 μM, and PD98059 at 1−20 μM. In all experiments, the chemicals were added as a dissolved form in dimethylsulfoxide (DMSO), and the concentration of DMSO did not exceed 1% of the culture volume, a concentration that did not affect any cellular processes of HEp-2 cells.

**Statistical Analysis**

Data are presented as the mean ± standard deviation from three independent experiments. Statistical analysis was performed using Student's *t* test (SYSTAT, SigmaPlot version 11; Systat Software Inc., Chicago, IL, USA) to evaluate the statistical significance of the results.

Differences were considered significant when $P < 0.05$. Data with $P < 0.01$ are indicated with two asterisks, whereas data with P-values between 0.01 and 0.05 are indicated with a single asterisk.

## RESULTS

**Confirmation of TTSS1-Defective Mutant *V. parahaemolyticus* Strain**

Among the two TTSSs found in *V. parahaemolyticus*, the role of TTSS1 was specifically examined in this study. Since the *vcrD1* gene encodes a component of TTSS1 that is highly conserved in various Gram-negative bacteria [21], a TTSS1-deficient mutant of *V. parahaemolyticus* was made by deleting the *vcrD1* gene. The putative VcrD1 ORF (VP1622) was deleted from the genomic DNA of *V. parahaemolyticus*, as confirmed by PCR using primers VP1622A and VP1622D specific to the upstream and downstream regions of the deleted *vcrD1* ORF, respectively. As expected, a 3,490 bp PCR product was amplified from wild-type DNA, whereas a smaller PCR product of 1,406 bp was produced from *ΔvcrD1* mutant *V parahaemolyticus*, NK1 (Fig. 1B).

To confirm that the *ΔvcrD1* mutant *V. parahaemolyticus* strain NK1 lost the function of TTSS1, secreted proteins from the *ΔvcrD1* mutant were harvested and analyzed by Western blot using anti-VopQ Ab (Fig. 1C), clearly showing that secretion of VopQ was abolished in the NK1 strain.

**Role of TTSS1 in Bacterial Cytotoxicity to HEp-2 Cells**

Earlier studies have shown that *ΔtdhS ΔtdhA V. parahaemolyticus* induces apoptotic death of the epithelial cells and that TTSS1 plays an important role in this process [21, 23]. In the present study, we examined the role of TTSS1 in *V. parahaemolyticus*-induced death of

HEp-2 cells in a genetic background with wild-type *tdhS* and *tdhA* genes. HEp-2 cells were treated with wild-type *V. parahaemolyticus* or *ΔvcrD1 V. parahaemolyticus* at a MOI of 200 for various exposure times (2–12 h), and the cytotoxicity of the bacteria against HEp-2 cells was determined by LDH release assay (Fig. 2A). For wild-type *V. parahaemolyticus*, the percentage of LDH release gradually increased up to 85% as the incubation time increased. In contrast, the *ΔvcrD1* mutant strain showed an attenuated ability to induce LDH release from the HEp-2 cells at all time points of infection (<10%). This result clearly indicates that *V. parahaemolyticus* is able to induce death of HEp-2 cells and that TTSS1 is one the main factors responsible for its cytotoxicity.

To confirm that the dysfunction of TTSS1 in the *ΔvcrD1* mutant is derived from absence of the *vcrD1* gene, a complementation plasmid containing wild-type *vcrD1* gene was transformed into the *ΔvcrD1* mutant *V. parahaemolyticus*

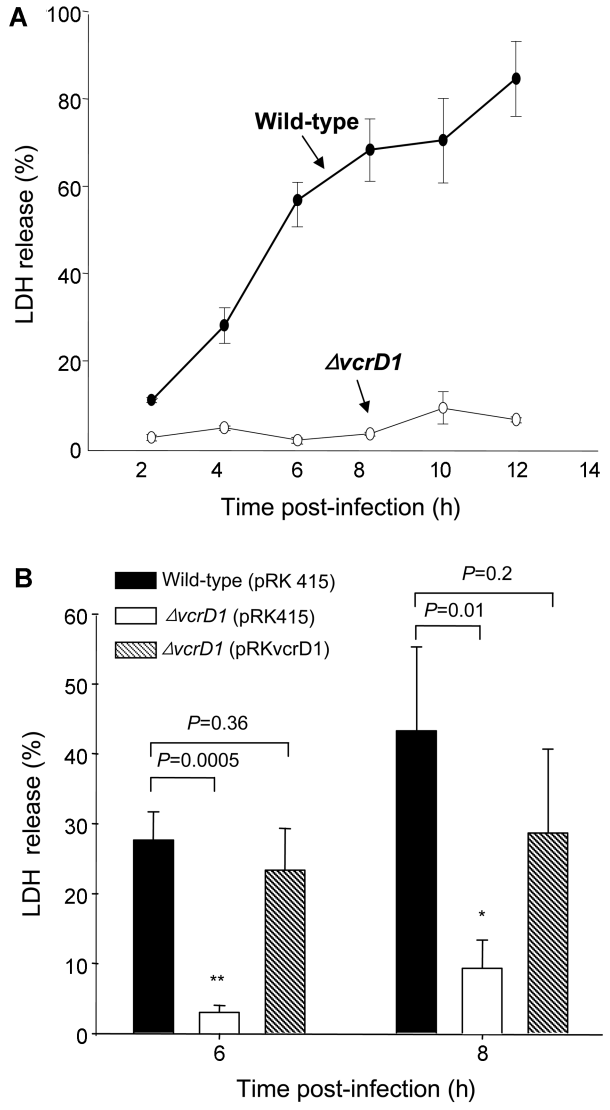


**Fig. 2.** Effect of *vcrD1* mutation on cytotoxicity of *V. parahaemolyticus* to HEp-2 cells.
**A**. The activity of LDH released from lysed HEp-2 cells was measured at various times of incubation (2–12 h) with wild-type (closed circle) or *ΔvcrD1 V. parahaemolyticus* (open circle) at MOI 200 using the CytoTox96 assay kit. **B**. Cytotoxicity of wild-type carrying pRK415 (closed bars), *ΔvcrD1* mutant NK1 carrying pRK415 (open bars), and NK1 carrying a complementation plasmid, pRKvcrD1 (hatched bars). HEp-2 cells ($1 \times 10^5$) were incubated with *V. parahaemolyticus* at MOI 200 for 6 h or 8 h. Data are shown with standard deviations for three independent experiments. Data with one or two asterisk(s) indicate that the cytotoxicity of NK1 carrying pRK415 was significantly reduced compared with that of wild-type carrying pRK415 with P-values = 0.01 or <0.01 (by Student's *t* test), respectively.

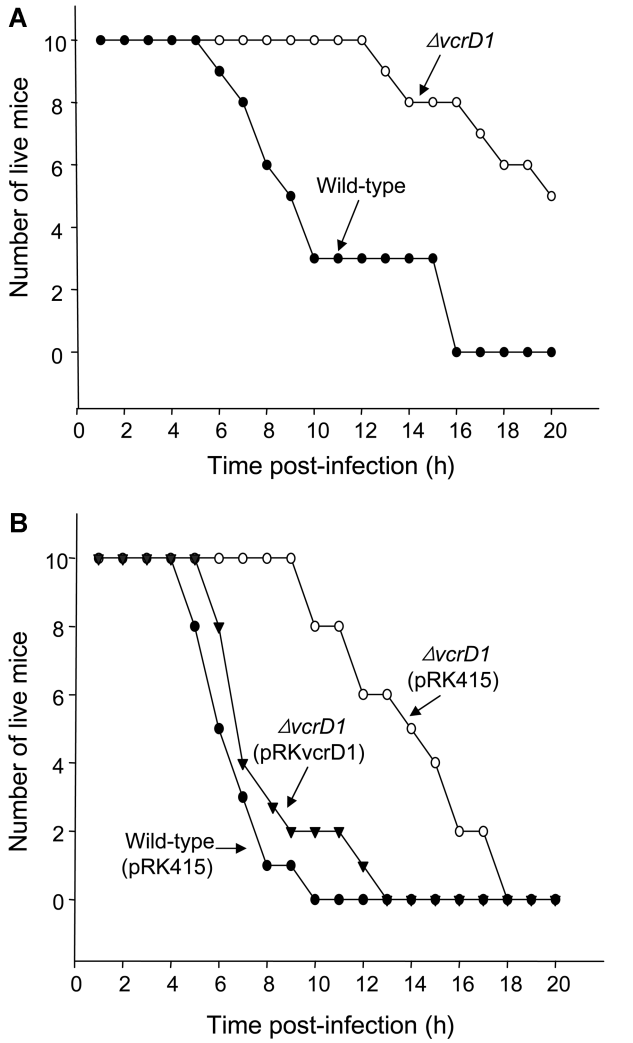


**Fig. 3.** Effect of TTSS1 on mouse lethality of *V. parahaemolyticus*.
Seven-week-old specific-pathogen-free female ICR mice were intraperitoneally infected with various *V. parahaemolyticus* strains: **A**. Wild-type (closed circles) or *ΔvcrD1* mutant *V. parahaemolyticus* strain (open circles); **B**. Wild-type carrying pRK415 (closed circles), *ΔvcrD1* carrying pRK415 (open circles), or *ΔvcrD1* with the complementation plasmid, pRKvcrD1 (closed inverted triangles). An equal number of bacteria ($1 \times 10^8$) was injected into 10 mice per group, and survival of the mice was monitored over 20 h following injection.

(Fig. 2B). Incubation with wild-type *V. parahaemolyticus* carrying the vector plasmid pRK415 at MOI 100 or 200 for 6 h resulted in 28% or 43% LDH release, respectively. The cytotoxicity of NK1 carrying pRK415 was low, but increased in a MOI-dependent manner (3% at MOI 100 versus 9% at MOI 200). We then examined whether the decreased cytotoxicity of the *DvcrD1* mutant could be recovered by the introduction of a complementation plasmid, pRKvcrD1. Inclusion of the complementation plasmid in the *ΔvcrD1* mutant increased LDH activity up to 67–82% of that of the wild-type strain carrying pRK415.

### Effect of *vcrD1* Mutation on *V. parahaemolyticus* Virulence in Mice

The role of *V. parahaemolyticus* TTSS1 in mouse lethality was then examined. Wild-type or *ΔvcrD1* mutant *V. parahaemolyticus* was injected intraperitoneally into 10 female mice at a dose of $1.0 \times 10^8$ bacterial cells per mouse and the number of live mice was determined over a 20 h period following infection (Fig. 3A). Compared with mice infected with wild-type *V. parahaemolyticus*, mice infected with the *ΔvcrD1* mutant showed a significant reduction in lethality; all 10 mice infected with wild-type bacteria were dead at 16 h post-injection, whereas five of the 10 NK1-infected mice were still viable at 20 h post-injection.

The virulence of complemented and control *V. parahaemolyticus* strains was also tested in the mouse model (Fig. 3B). Mice infected with the *ΔvcrD1* mutant carrying pRK415 were slowly dead until 18 h post-injection. Mice inoculated with wild-type *V. parahaemolyticus* carrying pRK415 were all dead at 10 h post-infection. Although the complemented strain (the *ΔvcrD1* mutant carrying pRKvcrD1) was efficient at killing mice, it was slightly less effective than wild-type *V. parahaemolyticus* carrying the vector plasmid pRK415, suggesting that introduction of plasmid containing the wild-type *vcrD1* gene into the *ΔvcrD1* mutant caused a partial, but significant, recovery of bacterial virulence in mice.

### Activation of MAPK Pathway in HEp-2 Cells upon *V. parahaemolyticus* Infection

MAPK is one of the main kinases triggering cellular responses to pathogenic organisms and is subdivided into three different forms; p38, ERK1/2, and JNK MAPKs [13]. We determined whether incubation of HEp-2 cells with *V. parahaemolyticus* triggers the activation of these three MAPKs. HEp-2 cells were incubated with wild-type *V. parahaemolyticus* for 6 h at various MOIs (10, 50, 100, and 200) and analyzed for the presence of phosphorylated forms of these MAPKs (Fig. 4A). p38 MAPK was indeed

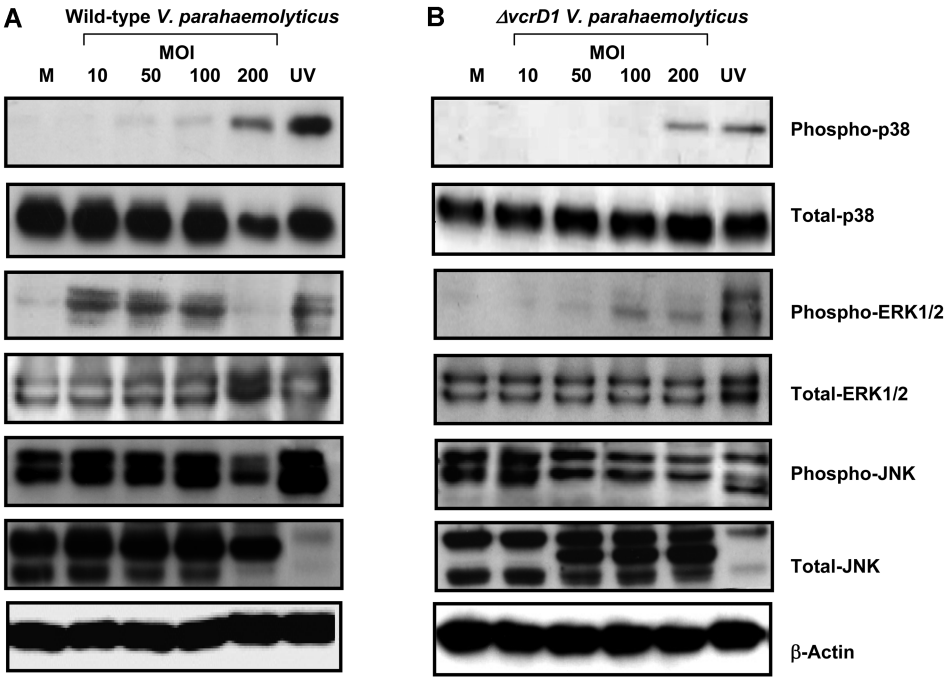


**Fig. 4.** Activation of MAPKs in *V. parahaemolyticus*-exposed HEp-2 cells.
Cell extracts were prepared from HEp-2 cells following incubation for 6 h with various MOIs (10–200) of wild-type *V. parahaemolyticus* (**A**) or *ΔvcrD1* mutant NK1 (**B**). Phosphorylated p38, phosphorylated ERK1/2, and phosphorylated JNK were measured by Western blotting. The membranes were stripped and reprobed for the p38, total ERK1/2 MAPK, and total JNK. Lane 1, medium only (M); lane 2, *V. parahaemolyticus*, MOI 10; lane 3, *V. parahaemolyticus*, MOI 50; lane 4, *V. parahaemolyticus*, MOI 100; lane 5, *V. parahaemolyticus*, MOI 200; lane 6, UV treatment, 30 min. The amount of β-actin was monitored as a loading control.

phosphorylated in cells incubated with wild-type *V. parahaemolyticus*, compared with cells treated with medium alone (negative control). The degree of p38 activation was proportional to the MOI of the bacteria. On the other hand, the amount of phosphorylated ERK1/2 induced by wild-type *V. parahaemolyticus* was maximal at the lower MOI of 10 and gradually decreased with increasing MOI of 50, 100, and 200. In contrast, exposure of HEp-2 cells to *V. parahaemolyticus* did not cause an increase in phosphorylation of JNK. Lysates prepared from HEp-2 cells that were treated with UV for 30 min served as a positive control for activation of the three MAPKs. The level of β-actin was also monitored in all of the cell lysates as a loading control for the amount of protein in each lane.

In the case of NK1, the *ΔvcrD1* mutant of *V. parahaeomolyticus*, the ability to trigger activation of p38 and ERK1/2 was reduced; although maximal activation of p38 and ERK1/2 was observed at MOIs of 200 and 100, respectively, the level of activation was lower than that in HEp-2 cells treated with wild-type bacteria.

### Role of MAPK Activation in *V. parahaemolyticus*-Induced Death of HEp-2 Cells

In subsequent experiments, we examined whether activation of MAPKs is important in *V. parahaemolyticus*-induced cell death. HEp-2 cells were pretreated with various concentrations (1 to 20 μM) of one of the selective MAPK inhibitors prior to incubation with wild-type *V. parahaemolyticus*. Bacterial cytotoxicity to HEp-2 cells was then monitored by measuring LDH release, and compared with LDH release from HEp-2 cells treated with DMSO.

HEp-2 cells pretreated with SB202190, a selective inhibitor of p38 MAPK, were incubated with wild-type *V. parahaemolyticus* and assayed for LDH release (Fig. 5A). Inactivation of p38 MAPK by SB202190 decreased *V. parahaemolyticus*-induced cell death in a dose-dependent manner to 66% of the control level (LDH release of DMSO-treated HEp-2 cells) at 20 μM. Similarly, pretreatment with PD98059 (a selective inhibitor of ERK1/2) prior to incubation with *V. parahaemolyticus* decreased the percentage of LDH release to 39% of the control at 20 μM PD98059 (Fig. 5B). In contrast, inactivation of JNK with SP600125 did not result in a decrease in *V. parahaemolyticus*-induced death of HEp-2 cells (Fig. 5C). This result suggests that among the three MAPKs, p38 and ERK1/2 are involved in *V. parahaemolyticus*-induced death of HEp-2 cells.

HEp-2 cells infected with the *ΔvcrD1* mutant *V. parahaemolyticus* showed a similar level of LDH release regardless of the presence of JNK or ERK1/2 inhibitor. However, LDH release induced by the NK1 strain decreased further to less than 7% in the presence of p38 inhibitor.

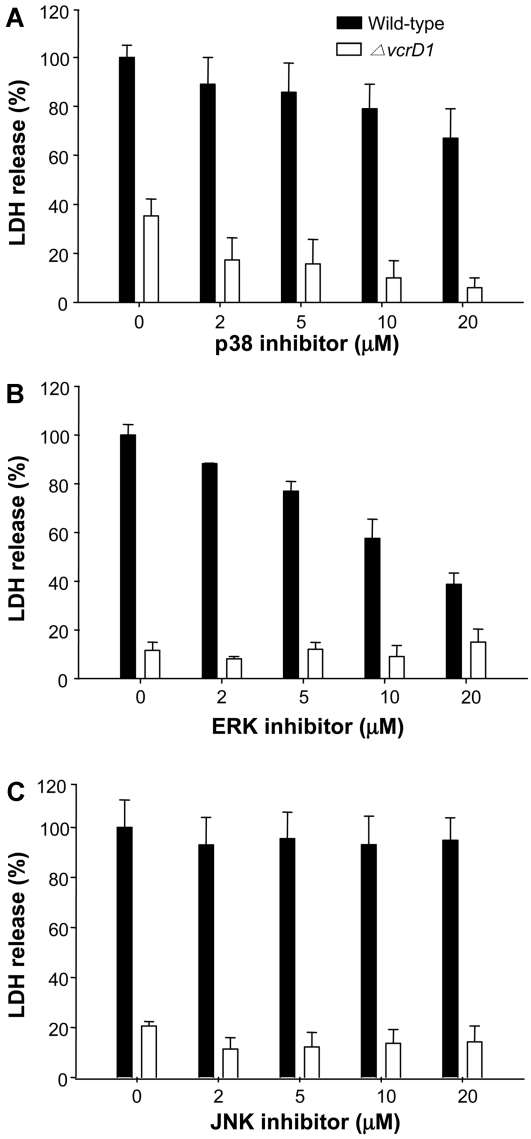


**Fig. 5.** Effects of MAPK inhibitors on *V. parahaemolyticus*-induced cytotoxicity.
HEp-2 cells were pretreated for 30 min with various concentrations (1–20 μM) of SB202190, a selective inhibitor of p38 MAPK (**A**); PD98509, a selective inhibitor of ERK1/2 (**B**); or SP600125, a selective inhibitor of JNK (**C**). The cells were then challenged with wild-type (closed bars) or *ΔvcrD1* mutant *V. parahaemolyticus* strain (open bars) for 6 h at MOI 200. Bacterial cytotoxicity was assayed by measuring LDH release into the culture supernatant. Results are representative of at least three independent experiments.

These data demonstrate that *V. parahaemolyticus* triggers activation of p38 and ERK1/2 in HEp-2 cells, eventually leading to cell death. Moreover, TTSS1 of *V. parahaemolyticus* has a differential effect on the two MAPKs, p38 and ERK1/2, with respect to cell death. That is, TTSS1 plays a significant role in ERK1/2-mediated cell death, whereas p38 functions independently from TTSS1 in this process.

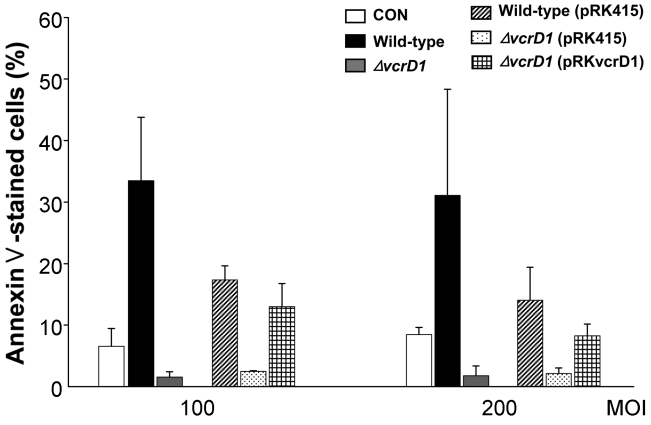


**Fig. 6.** Effect of *vcrD1* mutation on the ability of bacteria to induce apoptosis in HEp-2 cells.
HEp-2 cells were co-cultured with various *V. parahaemolyticus* strains (wild-type, *ΔvcrD* mutant NK1, wild-type carrying pRK415, NK-1 carrying pRK415, and NK-1 carrying pRKvcrD1) for 6 h at MOIs 100 and 200. Dead cells were detected by staining with annexin V at a concentration of 2 μg/ml, and the degree of cell death was assessed using FACS analysis of at least 10,000 cells per sample. Data are shown with standard deviation for three independent experiments.

### Measurement of Apoptosis of *V. parahemolyticus*-Infected HEp-2 Cells by Annexin V Staining

As a preliminary experiment to define the role of caspase(s) in *V. parahaemolyticus*-induced death of HEp-2 cells, we measured apoptosis in *V. parahaemolyticus*-exposed HEp-2 cells by staining with annexin V (Fig. 6). At a MOI 100 of wild-type *V. parahaemolyticus*, 33% of the HEp-2 cells were stained with annexin V, whereas only 2% were stained following treatment with the NK1 strain. The role of VcrD1 in *V. parahaemolyticus*-induced apoptosis of HEp2 was confirmed by a complementation experiment; addition of the complementation plasmid pRKvcrD1 into the NK1 strain increased the percentage of annexin-V-stained cells from 2% to 13%. In the case of wild-type *V. parahaemolyticus* carrying pRK415, 17% of the HEp-2 cells were stained with annexin V.

Infection of HEp-2 cells with various *V. parahaemolyticus* strains at MOI 200 resulted in similar levels of annexin V staining at infection with MOI 100. The absence of an increase in the number of apoptotic cells at a higher MOI may reflect the increased number of necrotic cells, which can be stained with propidium iodide (data not shown).

### Role of Caspase(s) in *V. parahaemolyticus*-Induced Death of HEp-2 Cells

Caspase activation is frequently considered synonymous with apoptotic cell death. Therefore, we investigated whether *V. parahaemolyticus* activates two caspases, caspase 3 and caspase 9, in HEp-2 cells (Fig. 7A and 7B, respectively). HEp-2 cells were incubated with *V. parahaemolyticus* for 6 h at various MOIs (from 10 to 200), and subjected to Western blot analysis using anti-caspase Abs. Activation of both caspase 3 and caspase 9 was clearly demonstrated by the appearance of smaller immunoreactive protein band(s) in the HEp-2 cells incubated with *V. parahaemolyticus*. HEp-2 cells treated with STS served as a positive control for caspase activation, showing degradation of both caspase 3 and caspase 9.

To examine whether caspase is involved in the *V. parahaemolyticus*-induced cell death, we treated HEp-2 cells with a pan-caspase inhibitor, z-VAD-FMK, and stained them with annexin V (Fig. 7C). z-VAD-FMK significantly protected STS-treated cells from death, indicating efficient inhibition of activation of caspases as previously reported [2]. However, the pan-caspase inhibitor did not prevent annexin V staining of HEp-2 cells infected with wild-type *V. parahaemolyticus.*

The caspase-independent nature of *V. parahaemolyticus*-induced cell death was also examined using an assay to measure LDH release (Fig. 7D). Consistent with the above results, treatment of HEp-2 cells with pan-caspase inhibitor did not affect LDH release upon infection with wild-type *V. parahaemolyticus*. Taken together, these data suggest that *V. parahaemolyticus*-induced cell death is a caspase-independent process.

## Discussion

Protein secretion is a key factor in the interaction of pathogenic bacteria with host cells. The type III secretion system is considered a virulence determinant, since proteins secreted through this system act directly with host cell components to alter its immune and cellular responses against the pathogens [11]. Genomic sequencing of *V. parahaemolyticus* revealed the presence of two TTSSs, which are involved in translocation of microbial factors into the cytoplasm of the host cells [21, 23]. Most previous studies on the role of these systems in the pathogenesis of *V. parahaemolyticus* have been performed in strains lacking its main virulence factor, TDH. This study aimed to define the role of TTSS1 in the *V. parahaemolyticus*–host interaction using *V. parahaemolyticus* in which TDHs are functional. In this study, we determined the cytotoxicity and mouse lethality of wild-type *V parahaemolyticus* and defined the function of two main signaling pathways, MAPK and caspase, in *V. parahaemolyticus*-induced death of the host cells. By comparing the ability of wild-type and TTSS1-defective *V. parahaemolyticus* bacteria to kill the host cells and activate these signaling pathways, we evaluated the involvement of TTSS1 effector(s) in these processes.

The attenuated virulence of the *ΔvcrD1* mutant *V. parahaemolyticus* in both *in vitro* and mouse models was

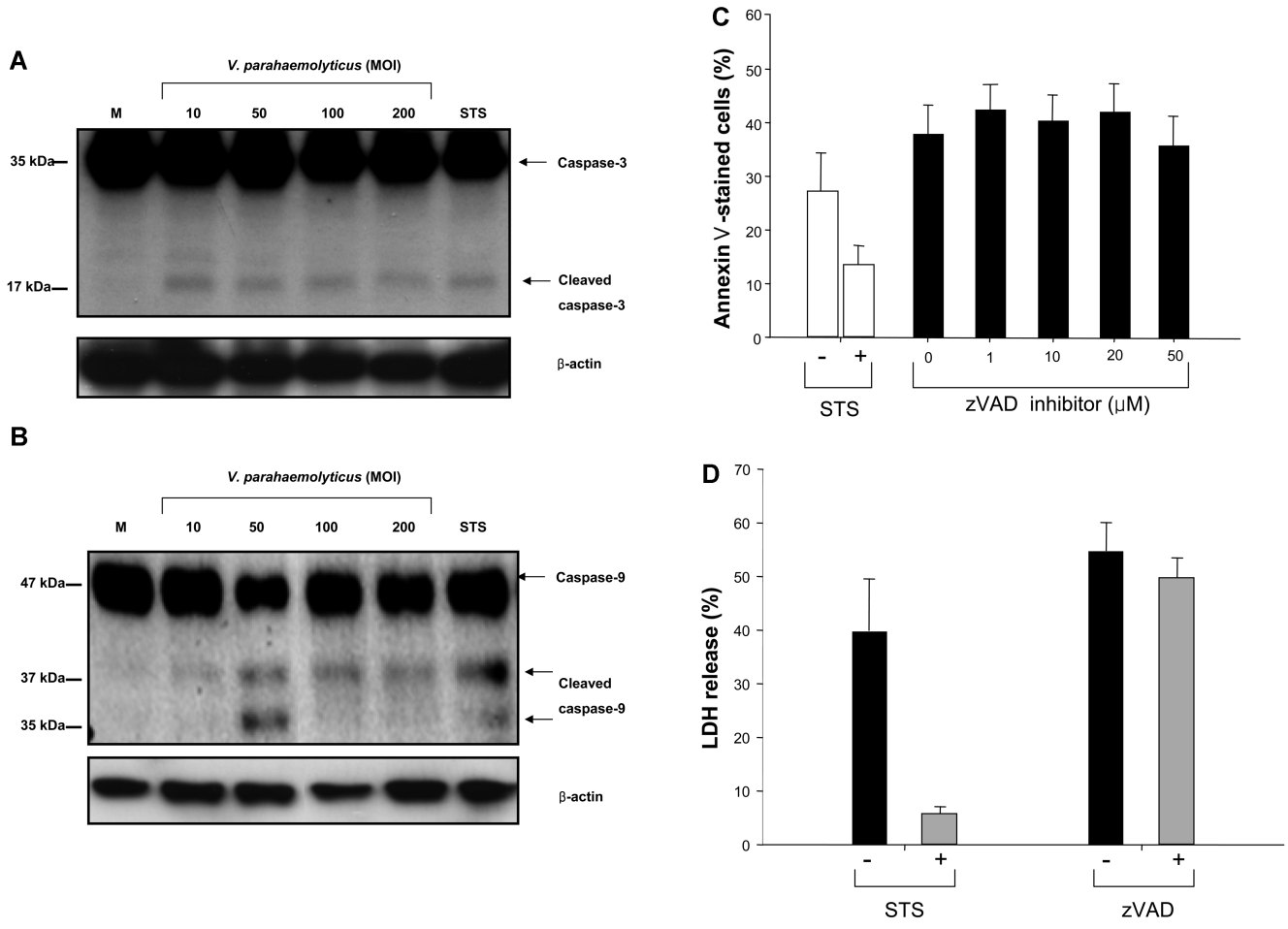


**Fig. 7.** Role of caspase in *V. parahaemolyticus*-induced death of HEp-2 cells.
**A**. Activation of caspase 3 in HEp-2 cells treated with *V. parahaemolyticus*. **B**. Activation of caspase 9 in HEp-2 cells treated with *V. parahaemolyticus*. HEp-2 cells were incubated for 6 h with wild-type *V. parahaemolyticus* at various MOIs (10–200) and analyzed by Western blot using anti-caspase Abs. HEp-2 cells were treated with 5 μM STS for 30 min to serve as a positive control for caspase activation. **C**. Effect of the pan-caspase inhibitor, z-VAD-FMK, on *V. parahaemolyticus*-induced apoptosis of HEp-2 cells. HEp-2 cells were treated with various concentrations (1–50 μM) of z-VAD-FMK prior to incubation with wild-type *V. parahaemolyticus* for 6 h at MOI 100. As a control, HEp-2 cells were treated with 1% DMSO before incubation with *V. parahaemolyticus*. HEp-2 cells treated with 5 μM STS were included as a positive control to confirm the activity of pan-caspase inhibitor. Apoptotic cells were detected by annexin-V staining. FACS analyses were performed on at least 10,000 cells per sample with a FACScan. Results are representative of at least three independent experiments. **D**. Effect of the pan-caspase inhibitor z-VAD-FMK on *V. parahaemolyticus*-induced LDH release of HEp-2 cells. HEp-2 cells were treated with 100 μM z-VAD-FMK prior to incubation with wild-type *V. parahaemolyticus* for 6 h at MOI 100. As a control, HEp-2 cells were treated with 1% DMSO before incubation with *V. parahaemolyticus*. HEp-2 cells treated with 5 μM STS were included as a positive control to monitor the activity of pan-caspase inhibitor. LDH activity released from lysed HEp-2 cells was measured using a CytoTox96 assay kit as described.

restored fully or partially when a *vcrD1*$^{+}$-plasmid was maintained in the mutant (Fig. 2B and 3B, respectively), indicating that VcrD1 is one of the main components of TTSS1. The importance of VcrD1 in TTSS1 was also confirmed by the defectiveness of VopQ secretion by the *ΔvcrD1* mutant of *V. parahaemolyticus* (Fig. 1C).

Since the *V. parahaemolyticus* strains used in this study retain wild-type loci of the *tdhS* and *tdhA* genes, secretion of TDHs is an important issue that should be addressed. However, TDHs have been shown to be secreted in a TTSS1- and TTSS2-independent manner and are postulated to be secreted *via* type II secretion system based on their putative signal peptide sequences [9]. Therefore, we can exclude the contribution of TDHs to the altered pathology demonstrated by the TTSS1-deficient *V. parahaemolyticus*.

Treatment with pan-caspase inhibitor did not affect the *V. parahaemolyticus*-induced LDH release and apoptosis of HEp-2 cells (Fig. 7C and 7D). Therefore, even though we observed activation of caspases in *V. parahaemolyticus*-exposed cells (Fig. 7A and 7B), their activation appears to be unrelated to the cytotoxicity of *V. parahaemolyticus*, which occurs through a caspase-independent mechanism. *V. parahaemolyticus*-induced cell death has been investigated in detail, and these earlier studies showed that TTSS1

induces rapid cell death initiated by acute autophagy in a caspase-independent manner [5, 6]. Specifically, VopQ, one of the TTSS1 effectors, is responsible for *V. parahaemolyticus*-induced autophagy [4]. In addition, another TTSS1 effector, VopS, is involved in apoptosis of macrophages *via* suppression of NF-kB activation [3] and is also implicated in cell rounding and collapse of the actin skeleton by direct inhibition of Rho family GTPase in HeLa cells [7]. Inhibition of Rho GTPase by VopS is mediated by covalent modification of Rho with adenosine 5'-monophosphate [31].

Among the three MAPKs, two MAPKs, p38 and ERK1/2, appeared to be important in *V. parahaemolyticus*-induced death (Fig. 5A and 5B). However, inhibitors of p38 or ERK1/2 differentially affected the cytotoxicity of the *ΔvcrD1* mutant *V. parahaemolyticus*. Treatment with p38 inhibitor decreased the cytotoxicity of both wild-type and the *ΔvcrD1* mutant, suggesting that the cytotoxic factor whose function is modulated by p38 MAPK is not secreted *via* TTSS1. On the other hand, the ERK1/2 inhibitor did not decrease cytotoxicity of the *ΔvcrD1* mutant, indicating that secretion of the cytotoxic factors controlled by ERK1/2 is mediated by TTSS1. Several proteins have been reported to be TTSS1 effectors, including VopQ (VP1680), VopR (VP1683), VopS (VP1686), and VopA (VPA1346) [21, 29]. Among these, VopA is a member of the family of YopJ-like proteins of *Yersinia* spp., which inhibits the MAPK and NF-kB signaling cascades resulting in inhibition of the host immune system [22]. *V. parahaemolyticus* YopA was shown to inhibit the MAPK pathway, but not the NF-kB pathway [30], and inhibition of MAPK was subsequently shown to occur *via* YopA-mediated acetylation of MAPK kinase [29]. Therefore, VopA may be the cytotoxic factor affected by MAPK inhibitors, but we cannot exclude involvement of other factors in the MAPK-mediated *V. parahaemolyticus*-induced death of HEp-2 cells.

In this study, we define the role of two host signaling pathways, caspase and MAPK, in *V. parahaemolyticus*-induced death of HEp-2 cells, and show that cytotoxicity is caspase-independent, ERK1/2-dependent, and p38-dependent. Moreover, the function of ERK1/2 in this process is mediated *via* TTSS1 effector(s). To fully understand the cytotoxicity of *V. parahaemolyticus*, extensive investigation should be performed on diverse microbial components, including secreted proteins, surface proteins, and effector proteins, of *V. parahaemolyticus*.

## Acknowledgment

This work was supported by a Korean Research Foundation Grant funded by the Korean Government (MOEHRD, Basic research Promotion Fund) (KRF-313-2008-2-C00798) to S.-J. P.

## References

1. Akeda, Y., K. Okayama, T. Kimura, R. Dryselius, T. Kodama, K. Oishi, T. Iida, and T. Honda. 2009. Identification and characterization of a type III secretion associated chaperone in the type III secretion system 1 of *Vibrio parahaemolyticus*. *FEMS Microbiol. Lett.* **296:** 18–25.
2. Belmorkhtar, C. A., J. Hillion, and E. Segal-Bendirdjian. 2001. Staurosporine induces apoptosis through both caspase-dependent and caspase-independent mechanisms. *Oncogene* **20:** 3354–3362.
3. Bhattacharjee, R. N., K. Park, Y. Kumagai, K. Okada, M. Yamamoto, S. Uematsu, *et al*. 2006. VP1686, a *Vibrio* type III secretion protein, induces Toll-like receptor-independent apoptosis in macrophage through NF-kB inhibition. *J. Biol. Chem*. **281:** 36897–36904.
4. Burdette, D. L., J. Seemann, and K. Orth. 2009. *Vibrio* VopQ induces PI3-kinase-independent autophagy and antagonizes phagocytosis. *Mol. Microbiol*. **73:** 639–649.
5. Burdette, D. L., M. L. Yarbrough, and K. Orth. 2009. Not without cause: *Vibrio parahaemolyticus* induces acute autophagy and cell death. *Autophagy* **5:** 100–102.
6. Burdette, D. L., M. L. Yarbrough, A. Orvedahl, C. J. Gilpin, and K. Orth. 2008. *Vibrio parahaemolyticus* orchestrates a multifaceted host cell infection by induction of autophagy, cell rounding, and then cell lysis. *Proc. Natl. Acad. Sci. USA* **105:** 12497–12502.
7. Casselli, T., T. Lynch, C. M. Southward, B. W. Jones, and R. DeVinney. 2008. *Vibrio parahaemolyticus* inhibition of Rho GTPase activation requires a functional chromosome I type III secretion system. *Infect. Immun*. **76:** 2202–2211.
8. Daniels, N. A., L. MacKinnon, R. Bishop, S. Altekruse, B. Ray, R. M. Hammond, *et al*. 2000. *Vibrio parahaemolyticus* infections in the United States, 1973–1998. *J. Infect. Dis*. **181:** 1661–1666.
9. Hiyoshi, H., T. Kodama, T. Iida, and T. Honda. 2010. Contribution of *Vibrio parahaemolyticus* virulence factors to cytotoxicity, enterotoxicity, and lethality in mice. *Infect. Immun*. **78:** 1772–1780.
10. Honda, T. and T. Iida. 1993. The pathogenicity of *Vibrio parahaemolyticus* and the role of the thermostable direct hemolysin and related hemolysin. *Rev. Med. Microbiol*. **4:** 106–113.
11. Hueck, C. J. 1998. Type III protein secretion systems in bacterial pathogens of animals and plants. *Microbiol. Mol. Biol. Rev.* **62:** 379–433.
12. Keen, N. T., S. Tamaki, D. Kobayashi, and D. Trollinger. 1998. Improved broad-host-range plasmids for DNA cloning in Gram-negative bacteria. *Gene* **70:** 191–197.
13. Kyosseva, S. V. 2004. Mitogen-activated protein kinase signaling. *Int. Rev. Neurobiol*. **59:** 201–210.
14. Liverman, A. D., H. C. Cheng, J. E. Trosky, D. W. Leung, M. L. Yarbrough, D. L. Burdette, *et al*. 2007. Arp2/3-independent assembly of actin by *Vibrio* type III effector VopL. *Proc. Natl. Acad. Sci. USA* **104:** 17117–17122.
15. Makino, K., K. Oshima, K. Kurokawa, K. Yokoyama, T. Uda, K. Tagomori, *et al*. 2003. Genome sequence of *Vibrio parahaemolyticus*: A pathogenic mechanism distinct from that of *V. cholerae*. *Lancet* **361:** 743–749.
16. Miller, V. L. and J. J. Mekalonos. 1988. A novel suicide vector and its use in construction of insertion mutations: Osmoregulation

of outer membrane proteins and virulence determinants in *Vibrio cholerae* requires *toxR*. *J. Bacteriol*. **170:** 2575–2583.
17. Milton, D. L., A. Norqvist, and H. Wolf-Watz. 1992. Cloning of a metalloprotease gene involved in the virulence mechanism of *Vibrio anguillarium*. *J. Bacteriol*. **174:** 7235–7244.
18. Morris Jr., J. G. 2003. Cholera and other types of vibriosis: A story of human pandemics and oysters on the half shell. *Clin. Infect. Dis.* **37:** 272–280.
19. Naim, R., I. Yanagihara, T. Iida, and T. Honda. 2001. *Vibrio parahaemolyticus* thermostable direct hemolysin can induce an apoptotic cell death in Rat-1 cells from inside and outside of the cells. *FEMS Microbiol. Lett*. **195:** 237–244.
20. Nair, G. B., T. Ramamurthy, S. K. Bhattacharya, B. Dutta, Y. Takeda, and D. A. Sack. 2007. Global dissemination of *Vibrio parahaemolyticus* serotype O3:K6 and its serovariants. *Clin. Microbiol. Rev.* **20:** 39–48.
21. Ono, T., K. S. Park, M. Ueta, T. Iida, and T. Honda. 2006. Identification of proteins secreted *via Vibrio parahaemolyticus* type III secretion system 1. *Infect. Immun.* **74:** 1032–1042.
22. Orth, K., L. E. Palmer, Z. Q. Bao, S. Stewart, A. E. Rudolph, J. B. Bliska, and J. E. Dixon. 1999. Inhibition of the mitogen-activated protein kinase kinase superfamily by a *Yersinia* effector. *Science* **285:** 1920–1923.
23. Park, K. S., T. Ono, M. Rokuda, M. H. Jang, K. Okada, T. Iida, and T. Honda. 2004. Functional characterization of two type III secretion systems of *Vibrio parahaemolyticus*. *Infect. Immun*. **72:** 6659–6665.
24. Raimondi, F., J. P. Kao, C. Fiorentini, A. Fabbri, G. Donelli, N. Gasparini, *et al*. 2000. Enterotoxicity and cytotoxicity of *Vibrio parahaemolyticus* thermostable direct hemolysin in *in vitro* systems. *Infect. Immun*. **68:** 3180–3185.
25. Tang, G. Q., T. Iida, K. Yamamoto, and T. Honda. 1995. $Ca^{2+}$-independent cytotoxicity of *Vibrio parahaemolyticus* thermostable direct hemolysin (TDH) on Intestine 407, a cell line derived from human embryonic intestine. *FEMS Microbiol. Lett*. **134:** 233–238.
26. Tang, G. Q., T. Iida, K. Yamamoto, and T. Honda. 1997. Analysis of functional domains of *Vibrio parahaemolyticus* thermostable direct hemolysin using monoclonal antibodies. *FEMS Microbiol. Lett.* **150:** 289–296.
27. Takahashi, A., T. Iida, R. Naim, Y. Naykaya, and T. Honda. 2001. Chloride secretion induced by thermostable direct hemolysin of *Vibrio parahaemolyticus* depends on colonic cell maturation. *J. Med. Microbiol*. **50:** 870–878.
28. Troisfontaines, P. and C. R. Cornelis. 2005. Type II secretion: More systems than you think. *Physiology* **20:** 326–339.
29. Trosky, J. E., Y. Li, S. Mukherjee, G. Keitany, H. Ball, and K. Orth. 2007. VopA inhibits ATP binding by acetylating the catalytic loop of MAPK kinases. *J. Biol. Chem.* **282:** 34299–34305.
30. Trosky, J. E., S. Mukherjee, D. L. Burdette, M. Roberts, L. McCarter, R. M. Siegel, and K. Orth. 2004. Inhibition of MAPK signaling pathways by VopA from *Vibrio parahaemolyticus*. *J. Biol. Chem.* **279:** 51953–51957.
31. Yarbrough, M. L., Y. Li, L. N. Kinch, N. V. Grishin, H. L. Ball, and K. Orth. 2009. AMPylation of Rho GTPases by *Vibrio* VopS disrupts effector binding and downstream signaling. *Science* **323:** 269–272.